

Original Research

# Decomposition of Organic Matter from Wastewater Using Ti/IrO<sub>2</sub>-RuO<sub>2</sub> Coated Electrodes: Electrode Characteristics and Removal Efficiency

Chunpeng Leng<sup>1</sup>, Yunxia Niu<sup>2,3</sup>, Yunlong Zhou<sup>2</sup>, Zhinian Yang<sup>2,3</sup>, Yue Yuan<sup>2,3</sup>,  
Fuping Li<sup>1\*</sup>, Hao Wang<sup>2,3,4\*\*</sup>

<sup>1</sup>College of Mining Engineering, North China University of Science and Technology, Tangshan, 063210, China

<sup>2</sup>College of Civil and Architectural Engineering, North China University of Science and Technology, Tangshan, 063210, China

<sup>3</sup>Key Laboratory of Bioelectrochemical Water Pollution Control Technology in Tangshan City, Tangshan, 063210, China

<sup>4</sup>Shaanxi Provincial Key Laboratory of Geological Support for Coal Green Exploitation, Xi'an University of Science and Technology, Xi'an, 710054, China

Received: 29 January 2022

Accepted: 28 February 2022

## Abstract

In this study, the preparation characteristics of coated electrodes were used to remove organic matter from wastewater. The effects of low concentration range in different current densities and pH on the removal of organic substances, chemical oxygen demand (COD) and ammonia nitrogen (NH<sub>3</sub>-N) by the coated electrode were explored. The experimental results indicated that the removal efficiency of NH<sub>3</sub>-N and COD achieved the optimum value when the electric current density was 8-10 mA/cm<sup>2</sup>, the pH value was mild alkaline or neutral, and the electrolysis time was about 30 min. The preparation process of coated electrode and the mechanism of degradation of organic matter in wastewater were investigated. The coated electrode was analyzed by blending Energy Dispersive X-Ray (EDX) and Scanning Electron Microscope (SEM). The results indicated that the titanium-based ruthenium coated electrode was more suitable for practical application.

**Keywords:** coating electrode, orthogonal experiment, scanning electron microscope

## Introduction

With the development of economy, China faced many environmental problems. The shortage of water resources and water environment pollution are the most essential issue [1]. As a new efficient and

environmental treatment technology, electrochemical technology had broaded attention by researchers [2-5]. As an environmentally friendly green technology, electrochemical technology was very effective for sewage treatment, and generally no secondary pollution [6-10].

Electrode was the core of electrochemical wastewater treatment technology. With the development of electrochemical technology and electrode coating

\*e-mail: crystal1689@126.com

\*\*e-mail: haowang1689@163.com

technology, a large number of alloys and new materials were used to explore the direction of electrode coating [11-14].

In simple terms, coated electrodes were coated or sprayed with some metal oxides on the substrate so that the resulting electrodes had better stability than the original electrode material. At present, the electrode matrix material was mainly based on titanium and brushed with precious metal materials, which made the electrode possess more stable physical characteristic and strengthen corrosion resistance properties to ensure that the electrode did not deform during electrolytic deposition process. Titanium-based coated electrode, also known as DSA anode, had the characteristics of high current density, good energy saving effect, long working life and relatively simple fabrication [15-17]. Titanium-based coated electrode could be used in many aspects of coating electrode electrolysis, such as chlor-alkali technology, seawater electrolysis, and waste water purification [18]. In addition, the shape of titanium-based coated electrodes was very malleable, with common shapes such as plates, grids, rods and tubes [19,20]. Considering the high efficiency and convenience of the electrode plate, the titanium-based coating electrode was prepared by using the mesh titanium substrate in this experiment. It was facilitated the operation and increased the effective contact area of the experiment.

In this study, the titanium-based ruthenium iridium coating materials were explored, and the ruthenium iridium coating was analyzed. SEM and EDX analysis showed that titanium-based ruthenium-iridium coating could enhance the stability of the electrode. In addition, the optimal experimental conditions were determined by orthogonal experiments to achieve higher energy utilization under certain energy consumption and improve the efficiency of electrode current. The elimination effect and dissociation mechanism of organic matter in wastewater by Ti-based ruthenium-iridium coating electrode were studied.

## Materials and Methods

### Preparation of Coated Electrodes

The titanium-based ruthenium-iridium electrode contained three metal elements. The ruthenium-iridium solution was stirred uniformly and then coated on the surface of the substrate. In this experiment, titanium-based ruthenium iridium coating electrode was prepared by thermal decomposition method [21]. The main process was shown in Fig. 1. Primarily, the clipping titanium mesh electrode substrate was polished with sandpaper, and then cleaned with ultrasonic for 10 minutes to remove organic contaminations on the superficialis of the titanium plate. Secondly, the n-butanol, isopropanol and concentrated hydrochloric acid solutions were uniformly mixed with the mixed solution of iridium chloride and ruthenium trichloride to prepare the coating solution. The coating solution was uniformly applied to the surface of the titanium plate to remove the external oxide layer with a soft brush. Dried in an oven of 80 degrees for 5 minutes, dried in a muffle furnace of 450 degrees and decompose for 5 minutes, then removed the titanium plate and cooled it to room temperature. Repeated this step 10 times. At this point, a uniform oxide coating was formed on the titanium substrate. Finally, the titanium substrate was brushed again and pyrolyzed in a muffle furnace for 1 hour. In order to make the coating more stable, the oxidation coating was completely oxidized.

### Experimental Device

Prepared  $\text{Ti}/\text{IrO}_2\text{-RuO}_2$  electrode was used as anode, and titanium plate was used as cathode. The test device was shown in Fig. 2. The effective volume of the diaphragm-less cell was 1 L. This experiment was powered by DC power supply and the effective area of the coating electrode was calculated. Since the selected coating electrode was cylindrical mesh, it was determined by counting that the electrode

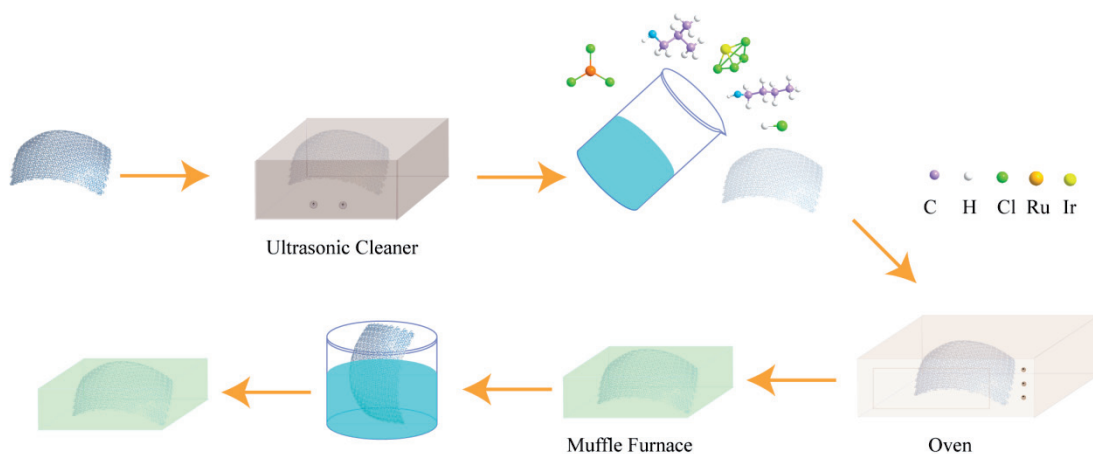


Fig. 1. Flowing chart for preparing coated electrodes.

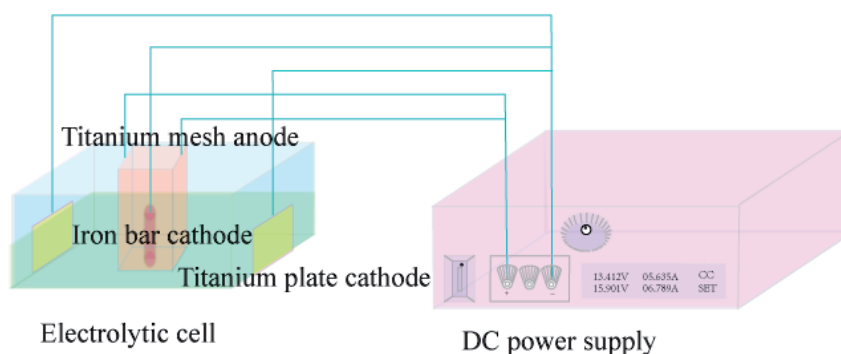


Fig. 2. Experimental setup.

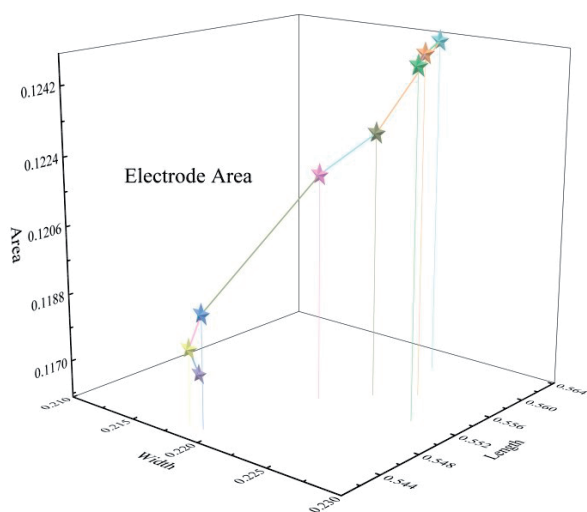


Fig. 3. Calculation of electrode area.

had about 600 holes and the shape of the hole was not exactly the same. Therefore, the calculations were considered and the following Fig. 3 was obtained after several measurements. The effective area of the cylindrical hole coating was calculated to obtain

an electrode radius of 4 cm and a height of 11 cm. However, in the actual electrolysis, the edge of the plate could not be completely washed, so 10 cm was taken as the effective height. The actual single surface area of the cylinder was calculated as  $251.2 - 73.2/2 = 214.6 \text{ cm}^2$ . Considering that the actual electrolysis process might not reach the maximum electrode efficiency and capillary phenomenon existed, the single surface area was chosen as  $200 \text{ cm}^2$  in the calculation [22]. The effective area ratio of cathode and anode was 3:1.

## Results and Discussion

### Analysis of Coating Electrode Properties

The most common determination method for testing the surface characteristics of coated electrodes was scanning electron microscopy [23]. SEM presented the information reflected by the secondary electron signal by means of an image tube monitor, which could easily, intuitively and effectively measure the surface morphology of the coating particles and the structure of the material in the coating [24, 25]. As shown in Fig. 4, the electrode surface coating roughness was moderate. The fluffy structure formed on the surface increased

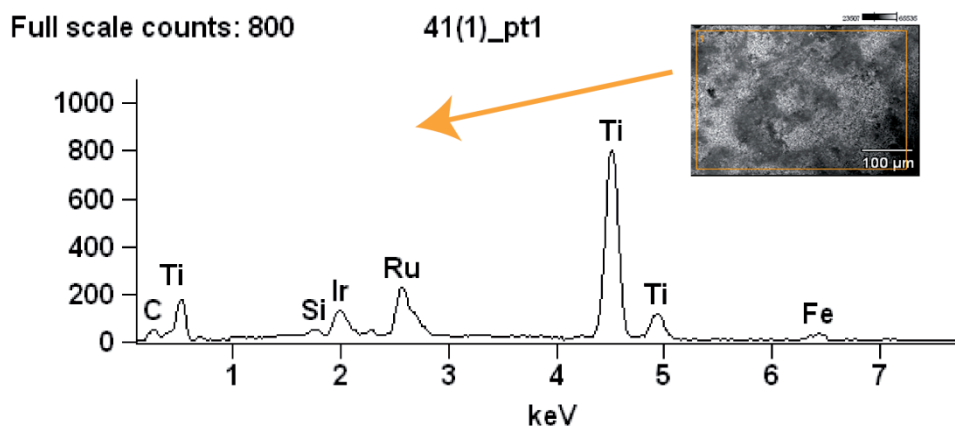


Fig. 4. SEM analysis and EDX analysis.

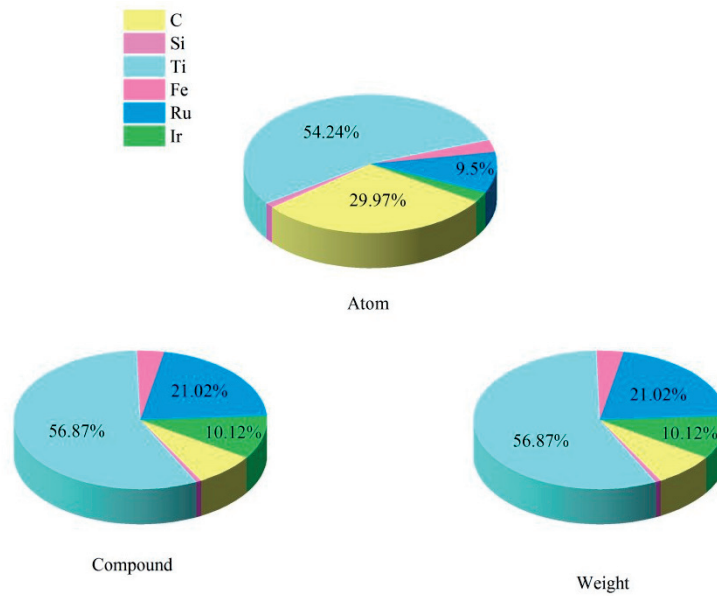


Fig. 5. Various components of the plate.

the surface area of the coated electrode and enhanced the reaction efficiency and electrode utilization [26]. The coating structure was stable, forming a layer of dense and uniform film, which could effectively prevent the electrolyte corrosion plate, prolong the service life of the electrode [27]. There were more obvious diffraction peaks under many diverse electron volt voltages. This phenomenon was attributed to the x-ray can directly contact the titanium substrate on the relatively thin coating, resulting in peak titanium. By comparing the diffraction apex with the standard peak, it could be seen

that the coating material was sufficient mixed and the fabric is tightly, which could protect the electrode plate.

As shown in Fig. 5, the maximum peak area of titanium as the substrate was also the most powerful, and the content was 56.87%. Ru accounted for 21.02% and Ir accounted for 10.12%. Titanium as matrix material not only had long service life, good chemical stability, but also had relatively low price [28]. Iridium was one of the coating material mixtures, and iridium metal had good ductility [29]. Ru was also widely applied in overlay materials, and its metal had excellent

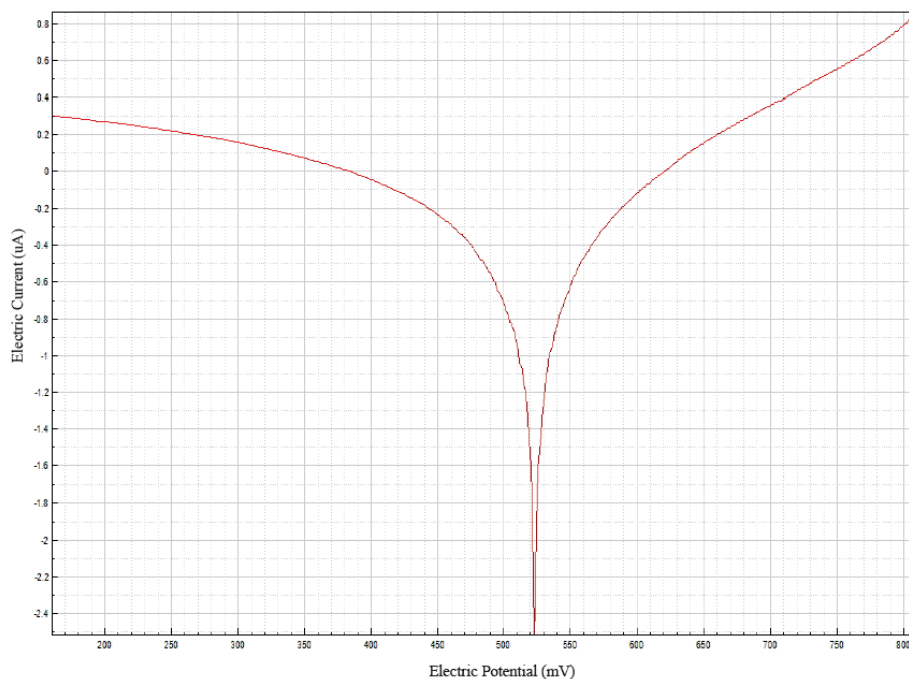


Fig. 6. Tafel curve.

Table 1. Orthogonal experiment form.

| Number of groups | Output current (A) | Current density (mA/cm <sup>2</sup> ) | Time (min) | pH |
|------------------|--------------------|---------------------------------------|------------|----|
| 1                | 1.2                | 6                                     | 15         | 3  |
| 2                | 1.2                | 6                                     | 30         | 5  |
| 3                | 1.2                | 6                                     | 45         | 7  |
| 4                | 1.2                | 6                                     | 60         | 9  |
| 5                | 1.6                | 8                                     | 15         | 5  |
| 6                | 1.6                | 8                                     | 30         | 3  |
| 7                | 1.6                | 8                                     | 45         | 9  |
| 8                | 1.6                | 8                                     | 60         | 7  |
| 9                | 2.0                | 10                                    | 15         | 7  |
| 10               | 2.0                | 10                                    | 30         | 9  |
| 11               | 2.0                | 10                                    | 45         | 3  |
| 12               | 2.0                | 10                                    | 60         | 5  |
| 13               | 2.4                | 12                                    | 15         | 9  |
| 14               | 2.4                | 12                                    | 30         | 7  |
| 15               | 2.4                | 12                                    | 45         | 5  |
| 16               | 2.4                | 12                                    | 60         | 3  |

electrocatalytic performance and could stably produce chlorine evolution reaction [30].

#### Electrochemical Analysis of Coated Electrodes

The titanium-based coating electrode used in this experiment was etched when the corrosion of the original battery, that was, this red-ox reaction was carried out on the titanium-based electrode [31]. Corrosion status of coating directly affected performance life of coating electrode [32]. As shown in Fig. 6, the electrochemical corrosion Tafel curve displayed that the corrosion potential of Ti/IrO<sub>2</sub>-RuO<sub>2</sub> electrode was 522 mV, and the potential was relatively higher than that of iron and zinc. Corrosion strength was much stronger than ordinary metal coating. Therefore, the coating material had wildly corrosion resistance and operation stability.

#### Determine the Values of Raw Water COD and NH<sub>3</sub>-N

##### Design Orthogonal Test Form

Orthogonal experiment explored the reaction degree of output current (1.2 A, 1.6 A, 2 A, 2.4 A), current density (6 mA/cm<sup>2</sup>, 8 mA/cm<sup>2</sup>, 10 mA/cm<sup>2</sup>, 12 mA/cm<sup>2</sup>) and pH (3, 5, 7, 9) at 15 min, 30 min, 45 min and 60 min, respectively. The four factors of output current, current density, time and degree of acidity and alkalinity were selected to determine the experimental data without considering the interaction. The purpose

was to save experimental time, save test materials and obtain the favorite experimental conditions. The orthogonal experiment table was shown in Table 1.

#### Determination of COD

As shown in Fig. 7, the chemical oxygen demand in water was determined by potassium dichromate method. At first, the ammonium ferrous sulfate solution was demarcated, and then the COD in the water sample was determined by reflux method. Three groups of parallel experiments were

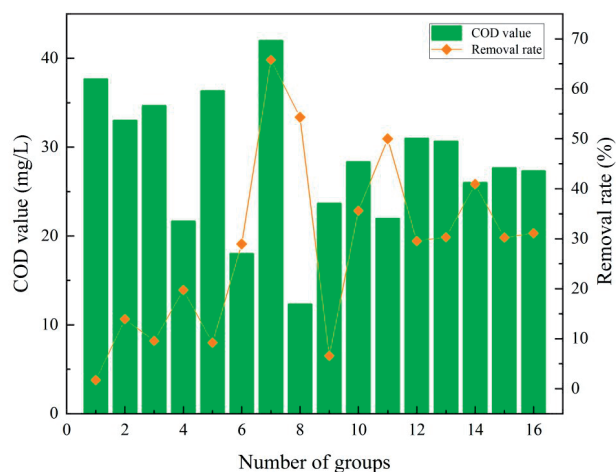


Fig. 7. COD removal rate.

conducted each time to ensure the stability of the data.

#### *Determination of Ammonia*

Nessler Reagent Spectrophotometry was applied for determination of  $\text{NH}_3\text{-N}$  in wastewater. As shown in Fig. 8, the first step was to test the chromogenic time. The second step was to draw the standard curve. Finally, the water sample was taken to determine the absorbance in the colorimetric tube, and the content of  $\text{NH}_3\text{-N}$  was determined by comparing the standard curve. Three blocks of parallel experiments were performed each time to guarantee the accuracy of the data.

#### *Degradation Mechanism*

The following conclusions could be obtained from Table 2:

(1) Under different electrolysis conditions, the amount of  $\text{NH}_3\text{-N}$  consumed by sewage was quite different [33]. When the influent was weakly alkaline or neutral, the removal rate of  $\text{NH}_3\text{-N}$  was the highest when the electrolysis time was about 30 minutes.  $\text{NH}_3\text{-N}$  existed in the form of ammonia molecules under alkaline conditions might be the reason. Nitrogen was easily generated by electrochemical reaction, and the concentration of  $\text{NH}_3\text{-N}$  reduced. It noticed that the electrolysis time of  $\text{NH}_3\text{-N}$  in biological sewage was not too long and more suitable for 30 minutes.

(2) The initial pH of the solution also affected the removal of  $\text{NH}_3\text{-N}$  [34]. Water was acidic when the

electrolysis, 15 minutes only consumed a small part of  $\text{NH}_3\text{-N}$ , but weak alkaline conditions,  $\text{NH}_3\text{-N}$  removal rate had been greatly improved. Therefore, weak alkaline environment could better promote the removal of  $\text{NH}_3\text{-N}$ .

(3) Current density for reducing the concentration of ammonia had a strong correlation. Theoretically, the higher the current density, the faster the ammonia reaction, and nitrogen removal rate should be higher. But in the actual electrolysis, the current density was too large, and energy consumption would increase significantly [6]. For practical applications, it had a greater impact. For the sake of synthesis, electrolysis should be carried out at a current of 8-10  $\text{mA}/\text{cm}^2$ , and energy consumption was relatively small.

The following conclusions can be drawn from Table 3:

(1) The change of electrolysis conditions had a great influence on the removal of COD. In the case of weak acidity and mild alkaline conditions, the COD consumption was large in about 45 minutes. If the electrolysis time was longer, the removal rate of organic matter in sewage had a certain degree of reduction, and prolonged electrolysis time would lead to the emergence of side effects in the electrolysis process. During the electrolysis there were a large number of bubbles and the whole water body had a certain temperature rise. For the COD part of the water, the electrolysis time should be kept at about 45 minutes. Weak acid and mild alkali had a positive effect on the reduction of COD concentration, which was not conducive to the reduction of COD concentration under powerful acid and alkaline conditions [35]. Especially in weak alkaline conditions,

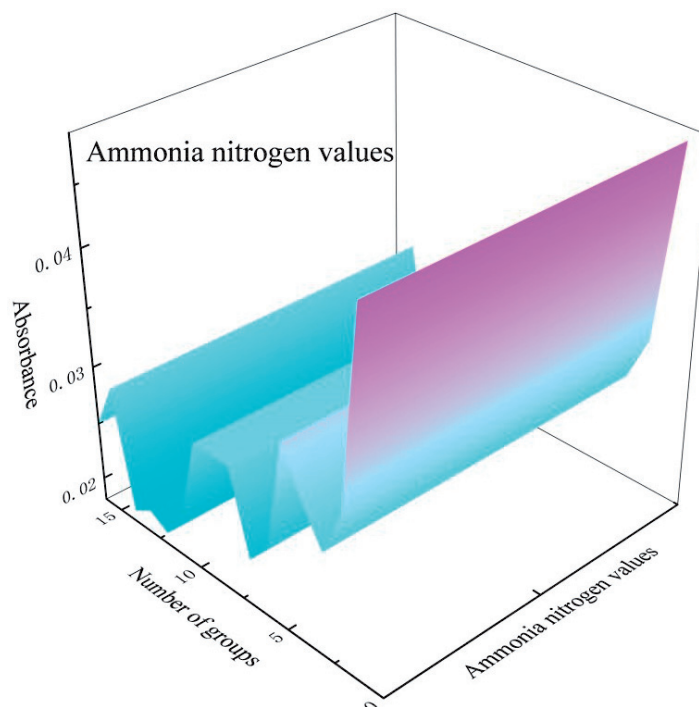


Fig. 8. Ammonia nitrogen values.

Table 2. NH<sub>3</sub>-N removal rate.

| Experiment number | Factor             |                                       |            |       |                                |                                 |
|-------------------|--------------------|---------------------------------------|------------|-------|--------------------------------|---------------------------------|
|                   | Output current (A) | Current density (mA/cm <sup>2</sup> ) | Time (min) | pH    | Ammonia nitrogen values (mg/L) | Ammonia nitrogen removal rate % |
| 1                 | 1.199              | 5.995                                 | 15         | 2.97  | 0.3747                         | 27.50                           |
| 2                 | 1.199              | 5.995                                 | 30         | 5.03  | 0.1550                         | 70.01                           |
| 3                 | 1.199              | 5.995                                 | 45         | 6.95  | 0.1034                         | 79.99                           |
| 4                 | 1.199              | 5.995                                 | 60         | 8.92  | 0.1421                         | 76.60                           |
| 5                 | 1.599              | 7.995                                 | 15         | 5.00  | 0.1938                         | 21.06                           |
| 6                 | 1.599              | 7.995                                 | 30         | 3.02  | 0.0646                         | 73.69                           |
| 7                 | 1.599              | 7.995                                 | 45         | 8.99  | 0.0388                         | 84.20                           |
| 8                 | 1.599              | 7.995                                 | 60         | 7.00  | 0.3876                         | 78.72                           |
| 9                 | 1.906              | 9.530                                 | 15         | 7.00  | 0.0904                         | 63.18                           |
| 10                | 1.999              | 9.995                                 | 30         | 8.95  | 0.0678                         | 47.37                           |
| 11                | 1.999              | 9.995                                 | 45         | 2.98  | 0.0388                         | 84.20                           |
| 12                | 1.999              | 9.995                                 | 60         | 4.99  | 0.0000                         | 100.00                          |
| 13                | 1.843              | 9.215                                 | 15         | 8.99  | 0.0129                         | 94.75                           |
| 14                | 1.994              | 9.97                                  | 30         | 7.01  | 0.0000                         | 100.00                          |
| 15                | 2.399              | 11.995                                | 45         | 5.00  | 0.1292                         | 47.37                           |
| 16                | 2.399              | 11.995                                | 60         | 2.98  | 0.0775                         | 68.43                           |
| K1                | 2.541              |                                       | 2.065      | 2.538 | 13.713                         |                                 |
| K2                | 2.577              |                                       | 2.911      | 2.384 |                                |                                 |
| K3                | 2.948              |                                       | 2.958      | 3.219 |                                |                                 |
| K4                | 3.106              |                                       | 3.238      | 3.029 |                                |                                 |
| $\overline{K1}$   | 0.635              |                                       | 0.516      | 0.635 | 1.143                          |                                 |
| $\overline{K2}$   | 0.644              |                                       | 0.728      | 0.596 |                                |                                 |
| $\overline{K3}$   | 0.737              |                                       | 0.740      | 0.805 |                                |                                 |
| $\overline{K4}$   | 0.777              |                                       | 0.810      | 0.757 |                                |                                 |
| R                 | 0.135              |                                       | 0.294      | 0.209 |                                |                                 |

the removal rate of chemical oxygen demand was the highest. In consequence, in order to save cost, the initial acidity and alkalinity of sewage should be appropriately improved in the application.

(2) Current density was closely related to COD removal. With the increase of current density, COD removal rate increased significantly. This indicated that high current density had a certain promoting effect on COD removal by electrolysis. But when the current density exceeded a certain limit, COD removal rate increased slowly. The reason was that under high current density, the liquor temperature rose, very large part of the energy generated by the electrode generated heat, resulting in decreased energy efficiency of the manufacturing equipments [36].

The current density should not be infinitely expanded to prolong the operating life of the electrode.

## Conclusions

Titanium-based ruthenium iridium coating electrode Ti/RuO<sub>2</sub>-IrO<sub>2</sub> as anode had many advantages such as long service life, stable property and strong anti-oxidation ability. The change of experimental conditions had great influence on the degradation of organic matter in wastewater, among them, the weak alkaline, relatively high current density and proper electrolysis time, had a good effect on the electrolysis experiment. The data obtained by orthogonal experiment could

Table 3. COD removal rate.

| Experiment number | Factor             |                                       |           |       |                  |                    |
|-------------------|--------------------|---------------------------------------|-----------|-------|------------------|--------------------|
| Number of groups  | Output current (A) | Current density (mA/cm <sup>2</sup> ) | Tme (min) | PH    | COD value (mg/L) | COD removal rate % |
| 1                 | 1.199              | 5.995                                 | 15        | 2.97  | 37.6667          | 1.74               |
| 2                 | 1.199              | 5.995                                 | 30        | 5.03  | 33.0000          | 13.91              |
| 3                 | 1.199              | 5.995                                 | 45        | 6.95  | 34.6667          | 9.57               |
| 4                 | 1.199              | 5.995                                 | 60        | 8.92  | 21.6667          | 19.75              |
| 5                 | 1.599              | 7.995                                 | 15        | 5.00  | 36.3333          | 9.21               |
| 6                 | 1.599              | 7.995                                 | 30        | 3.02  | 18.0000          | 28.95              |
| 7                 | 1.599              | 7.995                                 | 45        | 8.99  | 42.0000          | 65.79              |
| 8                 | 1.599              | 7.995                                 | 60        | 7.00  | 12.3333          | 54.32              |
| 9                 | 1.906              | 9.530                                 | 15        | 7.00  | 23.6667          | 6.58               |
| 10                | 1.999              | 9.995                                 | 30        | 8.95  | 28.3333          | 35.61              |
| 11                | 1.999              | 9.995                                 | 45        | 2.98  | 22.0000          | 50.00              |
| 12                | 1.999              | 9.995                                 | 60        | 4.99  | 31.0000          | 29.55              |
| 13                | 1.843              | 9.215                                 | 15        | 8.99  | 30.6667          | 30.30              |
| 14                | 1.994              | 9.970                                 | 30        | 7.01  | 26.0000          | 40.91              |
| 15                | 2.399              | 11.995                                | 45        | 5.00  | 27.6667          | 30.25              |
| 16                | 2.399              | 11.995                                | 60        | 2.98  | 27.3333          | 31.09              |
| K1                | 0.450              |                                       | 0.478     | 0.668 | 4.576            |                    |
| K2                | 1.583              |                                       | 1.194     | 1.194 |                  |                    |
| K3                | 1.217              |                                       | 1.556     | 1.556 |                  |                    |
| K4                | 1.326              |                                       | 1.347     | 1.515 |                  |                    |
| $\overline{K1}$   | 0.113              |                                       | 0.120     | 0.167 | 0.396            |                    |
| $\overline{K2}$   | 0.385              |                                       | 0.299     | 0.299 |                  |                    |
| $\overline{K3}$   | 0.304              |                                       | 0.389     | 0.389 |                  |                    |
| $\overline{K4}$   | 0.332              |                                       | 0.337     | 0.379 |                  |                    |
| R                 | 0.272              |                                       | 0.269     | 0.222 |                  |                    |

provide reference for the actual large-scale treatment of organic wastewater. Ti/RuO<sub>2</sub>-IrO<sub>2</sub> electrode was stable and efficient in the treatment of organic wastewater. When selected coating electrode materials, it had obvious advantages.

### Acknowledgments

This work was supported by Major Foundation of Hebei Educational Committee [ZD2021085], Tangshan science and technology innovation team training plan [19130208C], Natural Science Foundation of Hebei Province [E2021209112] and supported by Open Fund of Shaanxi Key Laboratory of

Geological Support for Coal Green Exploitation [NO. DZBZ2020-02].

### Conflict of Interest

The authors declare no conflict of interest.

### References

1. CHEN Y.Z., LU H.W., YAN P.D., YANG Y.Y., LI J. Analysis of water-carbon-ecological footprints and resource-environment pressure in the triangle of central china. *Ecol. Indic.* **125**, 107448, 2021.

2. CHEN S., CHEN W., WANG X., DING Y., WANG J. Treating simulated nitrate pollution groundwater with different pH by microbial fuel cell. *Pol. J. Environ. Stud.* **29** (6), 4007, **2020**.
3. WANG H., QUAN B.X., BO G.Z., ZHANG Y.Z., LIU L., ZHANG J.S., ZHANG X.Y., ZHANG C.H. Advanced oxidation treatment of dissolved organic matter from wastewater treatment plant secondary effluent using scattering electrical reactor. *J. Cleaner Prod.* **267**, 122258, **2020**.
4. SANTOS I.D., DEZOTTI M., DUTRA A.J.B. Electrochemical treatment of effluents from petroleum industry using a Ti/RuO<sub>2</sub> anode. *Chem. Eng. J.* **226** (12), 293, **2013**.
5. ROCHA J.H.B., GOMES M.M.S., FEMANDES N.S., SILVA D.R.D., MARTINEZ C.A. Application of electrochemical oxidation as alternative treatment of produced water generated by Brazilian petrochemical industry. *Fuel Process. Technol.* **96** (2), 80, **2012**.
6. WANG H., WANG J., BO G. Z., WU S.R., LUO L.T. Degradation of pollutants in polluted river water using Ti/IrO<sub>2</sub>-Ta<sub>2</sub>O<sub>5</sub> coating electrode and evaluation of electrode characteristics. *J. Cleaner Prod.* **273**, 123019, **2020**.
7. DAS N., MADHAVAN J., SELVI A., DAS D. An overview of cephalosporin antibiotics as emerging contaminants: a serious environmental concern. *Biotech.* **9** (6), 231, **2019**.
8. HASSEN T., NASR B., ABDELLATIF G. Anodic oxidation of aqueous wastes containing hydroquinone on BDD electrode. *Journal of advanced oxidation technology.* **18** (1), 155, **2015**.
9. SANTOS D., PACHECO M.J., GOMES A., LOPES A. Preparation of Ti/Pt/SnO<sub>2</sub>-Sb<sub>2</sub>O<sub>4</sub> electrodes for anodic oxidation of pharmaceutical drugs. *J. Appl. Electrochem.* **43** (4), 407, **2013**.
10. OTURAN M.A., AARON J.J. Advanced Oxidation Processes in Water/Wastewater Treatment: Principles and Applications. A Review. *Critical Reviews in Environmental Science and Technology.* **44** (23), 2577, **2014**.
11. KIM N., KIM Y., PARK J.B., CHO H.H., LEE D.K., KWAK G., YU H.K. Micro-networked metal coating using self-cracked WO<sub>3</sub> inorganic thin film as sacrificial layer: application to transparent flexible electrodes. *Thin Solid Films.* **736**, 138916, **2021**.
12. KONG Y., WANG Z.L., WANG Y., YUAN J., CHEN Z.D. Degradation of methyl orange in artificial wastewater through electrochemical oxidation using exfoliated graphite electrode. *New Carbon Mater.* **26** (6), 459, **2011**.
13. PASTEFANAKIS N., MANTZAVINOS D., KATSAOUNIS A. DSA electrochemical treatment of olive mill wastewater on Ti/RuO<sub>2</sub> anode. *J. Appl. Electrochem.* **40** (4), 729, **2010**.
14. LUO Y.J., CHEN A., XU M., CHEN D.X., TANG J., MA D., ZHANG H.Z. Preparation, characterization, and in vitro/vivo evaluation of dexamethasone/poly( $\epsilon$ -caprolactone)-based electrode coatings for cochlear implants. *Drug delivery.* **28** (1), 1960927, **2021**.
15. ESPINOZA L.C., SEPÚLVEDA P., GARCÍA A., GODOI D.M., SALAZAR R. Degradation of oxamic acid using dimensionally stable anodes (DSA) based on a mixture of RuO<sub>2</sub> and IrO<sub>2</sub> nanoparticles. *Chemosphere.* **251**, 126674, **2020**.
16. COSTA C.R., BOTTA C.M.R., ESPINDOLA E.L.G., OLIVI P. Electrochemical treatment of tannery wastewater using DSA electrodes. *J. Hazard. Mater.* **153** (1-2), 616, **2008**.
17. JIANG N., ZHAO Q.L., XUE Y., XU W.J., XU Z.F.Y. Removal of dinitrotoluene sulfonate from explosive wastewater by electrochemical method using Ti/IrO<sub>2</sub> as electrode. *J. Cleaner Prod.* **188**, 732, **2018**.
18. YE F., LI J., WANG X., WANG T., LI S., WEI H. Electrocatalytic properties of Ti/Pt-IrO<sub>2</sub> anode for oxygen evolution in PEM water electrolysis. *Int. J. Hydrogen Energy.* **35** (15), 8049, **2010**.
19. TENG J., LIU G.S., LIANG J.B., YOU S.J. Electrochemical oxidation of sulfadiazine with titanium suboxide mesh anode. *Electrochim. Acta.* **331**, 135441, **2020**.
20. ZHANG Y.S., ZHANG C.L., LIU K.M., ZHU X., LIU F., GE X.F. Biologically synthesized titanium oxide nanostructures combined with morphogenetic protein as wound healing agent in the femoral fracture after surgery. *J. Photochem. Photobiol., B.* **182**, 35, **2018**.
21. ELMI F., YOUSEFI B., ELMI M.M., ALINEZHAD H., MOULANA Z. Thermal decomposition synthesis of Zn-HAP (extracted from fish scale) nanopowder and its photocatalytic and antibacterial activities under visible light. *Ceram. Int.* **47** (15), 21862, **2021**.
22. MERABIA S., BONET A., PAGONABARRAGA I. Modelling capillary phenomena at a mesoscale: from simple to complex fluids. *J. Non-Newtonian Fluid Mech.* **154** (1), 13, **2008**.
23. TANG Q.C., DAI X.Y., WANG Z.F., WU F.Z., MAI Y., GU Y.J., DENG Y. Enhanced high-voltage performance of LiCoO<sub>2</sub> cathode by directly coating of the electrode with Li<sub>2</sub>CO<sub>3</sub> via a wet chemical method. *Ceram. Int.* **47** (14), 19374, **2021**.
24. JIANG Z.Q., SUN D.Q., GUAN H.Z., SUN Y.T., YE M.L., ZHANG L., GU T.T., CHEN J.N. Transmission electron microscopy analysis on microbial ultrathin sections prepared by the ultra-low lead staining technique. *Microsc. Microanal.* **27** (5), 1265, **2021**.
25. LU T.L., DAI J.H., TIAN J.T., SONG W.W., LIU X.Z., LAI L., CHU H.J., HUANG X., LIU X.Y. Synthesis of Na<sub>0.5</sub>Bi<sub>0.5</sub>TiO<sub>3</sub> powders through hydrothermal method. *J. Alloys Compd.* **490**, 232, **2010**.
26. ZOU B.K., ZHANG Y.Y., WANG J.Y., LIANG X., MA X.H., CHEN C.H. Hydrothermally enhanced MnO/reduced graphite oxide composite anode materials for high performance lithium-ion batteries. *Electrochim. Acta.* **167**, 25, **2015**.
27. ZHANG Z.W., XIAO Q.G., DU X., XUE T.Y., YAN Z.P., LIU Z.F., ZHANG H., QI T. The fabrication of Ti<sub>4</sub>O<sub>7</sub> particle composite modified PbO<sub>2</sub> coating electrode and its application in the electrochemical oxidation degradation of organic wastewater. *J. Alloys Compd.* **897**, 162742, **2021**.
28. DUAN P.Z., HU X., JI Z.Y., YANG X.M., SUN Z.R. Enhanced oxidation potential of Ti/SnO<sub>2</sub>-Cu electrode for electrochemical degradation of low-concentration ceftazidime in aqueous solution: performance and degradation pathway. *Chemosphere.* **212**, 594, **2018**.
29. DONG L.L., ZHANG W., FU Y.Q., LU J.W., LIU Y., ZHANG Y. S. Synergetic enhancement of strength and ductility for titanium-based composites reinforced with nickel metallized multi-walled carbon nanotubes. *Carbon.* **184**, 583, **2021**.
30. LI J., QIN X., CHEN G., CHEN G. The effect of ruthenium content on the stability and activity of Ti/RuO<sub>2</sub>-Sb<sub>2</sub>O<sub>5</sub>-SnO<sub>2</sub> for oxygen evolution. *J. Taiwan Inst. Chem. Eng.* **125**, 186, **2021**.
31. PENG X.F., WANG C.H., LI Y.Y., MA H., YU F., CHE G.S., YAN J.Y., ZHANG X.T., LIU Y.C. Revisiting cocatalyst/

- TiO<sub>2</sub> photocatalyst in blue light photothermal catalysis. *Catal. Today*. **335**, 3594, **2019**.
32. JIN J., ZHANG J.Z., HU M. L., LI X. Investigation of high potential corrosion protection with titanium carbonitride coating on 316l stainless steel bipolar plates. *Corros. Sci.* **191**, 109757, **2021**.
  33. ZHENG D.C., GU W.Z., ZHOU Q.M., ZHANG L.X., WEI C.C., YANG Q.Z. M., LI D.P. Ammonia oxidation and denitrification in a bio-anode single-chambered microbial electrolysis cell. *Bioresour. Technol.* **310**, 123466, **2020**.
  34. BAN F.C., NAN H.D., JIN Q., DAI M.Y. Response surface methodology for optimizing the degradation of methyl orange in aqueous solution by a diaphragm system that utilizes a cathode and anode coaction electrochemical method. *Pol. J. Environ. Stud.* **31** (1), 1, **2022**.
  35. ZOU R., TANG K., HAMBLY A.C., WÜNSCH U.J., ANDERSEN H.R., ANGELIDAKI I., ZHANG Y. When microbial electrochemistry meets UV: The applicability to high-strength real pharmaceutical industry wastewater. *J. Hazard. Mater.* **423**, 127151. **2022**.
  36. ZHANG Z.W., HAN Y.X., XU C.Y., HAN H.J., ZHONG D., ZHENG M.Q., MA W.W. Effect of low-intensity direct current electric field on microbial nitrate removal in coal pyrolysis wastewater with low COD to nitrogen ratio. *Bioresour. Technol.* **287**, 121465, **2019**.